Biochemical Pharmacology 228 (2024) 116161

Contents lists available at ScienceDirect

Biochemical Pharmacology

journal homepage: www.elsevier.com/locate/biochempharm

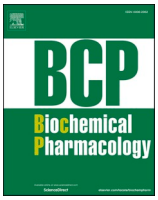

Targeting metabolic adaptive responses induced by glucose starvation inhibits cell proliferation and enhances cell death in osimertinib-resistant non-small cell lung cancer (NSCLC) cell lines

Kamal Eltayeb [a], Roberta Alfieri [a,*], Claudia Fumarola [a], Mara Bonelli [a], Maricla Galetti [b], Andrea Cavazzoni [a], Graziana Digiacomo [a], Francesca Galvani [c], Federica Vacondio [c], Alessio Lodola [c], Marco Mor [c], Roberta Minari [d], Marcello Tiseo [a,d], Silvia La Monica [a,1], Pier Giorgio Petronini [a,1]

[a] Department of Medicine and Surgery, University of Parma, 43126 Parma, Italy
[b] Department of Occupational and Environmental Medicine, Epidemiology and Hygiene, INAIL-Italian Workers' Compensation Authority, Monte Porzio Catone, 00078 Rome, Italy
[c] Department of Food and Drug, University of Parma, 43124 Parma, Italy
[d] Medical Oncology Unit, University Hospital of Parma, 43126 Parma, Italy

ARTICLE INFO

Keywords:
NSCLC
EGFR
Osimertinib
Resistance
Metabolism
Glucose

ABSTRACT

Osimertinib, a tyrosine kinase inhibitor targeting mutant EGFR, has received approval for initial treatment in patients with Non-Small Cell Lung Cancer (NSCLC). While effective in both first- and second-line treatments, patients eventually develop acquired resistance. Metabolic reprogramming represents a strategy through which cancer cells may resist and adapt to the selective pressure exerted by the drug. In the current study, we investigated the metabolic adaptations associated with osimertinib-resistance in NSCLC cells under low glucose culture conditions. We demonstrated that, unlike osimertinib-sensitive cells, osimertinib-resistant cells were able to survive under low glucose conditions by increasing the rate of glucose and glutamine uptake and by shifting towards mitochondrial metabolism. Inhibiting glucose/pyruvate contribution to mitochondrial respiration, glutamine deamination to glutamate, and oxidative phosphorylation decreased the proliferation and survival abilities of osimertinib-resistant cells to glucose starvation. Our findings underscore the remarkable adaptability of osimertinib-resistant NSCLC cells in a low glucose environment and highlight the pivotal role of mitochondrial metabolism in mediating this adaptation. Targeting the metabolic adaptive responses triggered by glucose shortage emerges as a promising strategy, effectively inhibiting cell proliferation and promoting cell death in osimertinib-resistant cells.

1. Introduction

Non-small cell lung carcinoma (NSCLC) represents the most common cause of cancer-related death in both men and women [1]. About 10–15 % of NSCLC cases were found to have mutations in the Epidermal Growth Factor Receptor (*EGFR)* tyrosine kinase domain such as in-frame deletion in exon 19 or point mutation in exon 21 (L858R mutation) [2]. Other mutations in *EGFR* include insertion within exon 20 which account for around 4 % [3]. The EGFR tyrosine kinase inhibitor (EGFR-TKI) osimertinib represents the first-line treatment for advanced NSCLC patients with *EGFR* mutations. It inhibits the mutated EGFR, as well as the secondary mutated EGFR T790M resistant to first and second-

Abbreviations: ASCT2, Alanine-Serine-Cysteine-Transporter-2; AMPK, 5′ Adenosine Monophosphate-activated Protein Kinase; DG, Deoxy-D-glucose; EGFR, Epidermal Growth Factor Receptor; GLS-1, Glutaminase-1; GLUT1, Glucose Transporter 1; LCFAs, Long-Chain Fatty Acids; MPC, Mitochondrial Pyruvate Carrier; NSCLC, Non-Small Cell Lung Cancer; OCR, Oxygen Consumption Rate; OXPHOS, Oxidative Phosphorylation; TCA, Tricarboxylic acid cycle; TKI, Tyrosine Kinase Inhibitor.

* Corresponding author.
E-mail address: roberta.alfieri@unipr.it (R. Alfieri).
[1] Co-last authors.

https://doi.org/10.1016/j.bcp.2024.116161
Received 10 January 2024; Received in revised form 12 March 2024; Accepted 21 March 2024
Available online 24 March 2024

generation EGFR-TKIs leading to improved outcomes [4]. However, despite high efficacy, resistance to osimertinib invariably develops and EGFR-dependent or independent mechanisms have been described [5–7]. While the role of genetic and epigenetic changes in osimertinib resistance is well understood, the role of metabolic reprogramming in the development or maintenance of resistance phenotypes remains to be defined.

Many alterations are known to be occurring in tumor cells to reprogram their metabolic profiles to ensure proliferation and survival. Adaptation in metabolic and energy pathways helps cancer cells to meet the increased demands for intermediates needed for the growth and proliferation of the primary tumor and redox balance maintenance as well as colonization of metastatic secondary sites [8].

Cancer cells reprogram their energy metabolism to favor aerobic glycolysis over oxidative phosphorylation (OXPHOS) leading to lactate accumulation even in oxygen presence (the so-called Warburg effect). EGFR signaling in NSCLC was found to enhance glycolysis not only for energy production but also for glycolytic intermediates production for synthetic processes such as synthesis of fatty acids, cholesterol, non-essential amino acids and ribulose-5-phosphate. The metabolic reprogramming to glycolysis induced by oncogenic mutated EGFR, may be reverted by EGFR-TKIs, contributing to cancer cell growth inhibition [9]. In osimertinib-sensitive cells, osimertinib reduced hexokinase1/2 activity and down-regulated the expression of other key regulators of glycolysis rendering them strongly dependent on OXPHOS metabolism for energy generation. Therefore, simultaneous treatment with osimertinib combined with phenformin delayed or prevented the emergence of resistance in both H1975 and PC9 cells [10]. Enhanced glycolysis induced by mutated EGFR is critical for EGFR stability through inhibiting autophagic EGFR degradation [11] and concomitant suppression of glycolysis and autophagy reverses osimertinib resistance in PC9 and H1975 cells [12].

Tumor cells encounter a variety of environmental challenges, including low oxygen levels (hypoxia), acidic conditions (acidosis), and limited access to essential nutrients due to an inadequate vascular network [13]. The scarcity of nutrients results from the heightened demand for rapid tumor growth, which often beats the available supply. Among these nutrient deficiencies, glucose shortage is the most prevalent, primarily because tumor cells consume glucose at a high rate, frequently reducing its concentration to less than 1 mM within solid tumor masses [14,15] To adapt to this glucose deficiency, tumor cells resort to alternative fuel sources such as lactate [16,17] by the enhancement in the activity of phosphoenolpyruvate carboxykinase 2, a key enzyme in the gluconeogenesis, and glutamine [18,19]. Glutamine is the most abundant amino acid in the blood; after its uptake, mediated by Alanine-Serine-Cysteine-Transporter-2 (ASCT2) and L-type Amino Acid Transporter, glutamine is converted into glutamate by Glutaminase-1 (GLS-1) and then glutamate is converted into α-ketoglutarate by the action of either glutamate dehydrogenase, aminotransferases, or asparagine synthetase which will lead to the biosynthesis of varied nitrogenous metabolites. Under low glucose concentrations, glutamine may maintain Tricarboxylic acid cycle (TCA) functions by acting as an anaplerotic substrate by providing α-ketoglutarate [20,21]. Cancer cells also employ strategies like breaking down their own cellular components through autophagy or utilizing resources from the surrounding microenvironment [13,22].

In the present study, we demonstrated that NSCLC osimertinib-resistant cells were able to survive under low glucose conditions through increasing the rate of glucose and glutamine uptake and shifting towards mitochondrial metabolism. Targeting these adaptive metabolic responses decreased proliferation and enhanced cell death of osimertinib-resistant cells.

2. Materials and methods

2.1. Cell culture

Human NSCLC cell line PC9, harboring *EGFR* exon 19 deletion, was provided by Dr. P. Jänne (Dana-Farber Cancer Institute, Boston, MA, USA), PC9T790M cell line (harboring the *EGFR* T790M secondary mutation) was generated in our laboratory by treating PC9 cells with increasing concentrations of gefitinib for 9 months [23].

The clones resistant to osimertinib, derived from osimertinib-sensitive PC9 or PC9T790M cells after long exposure to increasing drug concentrations, have different acquired mechanisms of resistance (either EGFR-dependent or EGFR-independent). PC9BRAFG469A cells with the G469A mutation [24]; PC9T790MclA with a still undefined EGFR-independent mechanism of resistance as previously reported [25]; PC9T790MC797S cells, kindly provided by Dr. M. Mancini, carry C797S *EGFR* mutation [26].

Cells were cultured in RPMI-1640 (Life Technologies, Gaithersburg, MD, USA) medium, supplemented with 10 % fetal bovine serum (Invitrogen, Carlsbad, CA, USA), 2 mM glutamine and 1 % of antibiotics (penicillin 100 U/ml and streptomycin 100 ug/ml). All cells were cultured and maintained under standard cell culture conditions at 37 °C in a water-saturated atmosphere of 5 % CO_2 and 95 % air. Resistant clones were routinely cultured in the presence of 500 nM osimertinib to maintain resistance during propagation.

2.2. Drug treatment

Osimertinib, was provided by AstraZeneca (Milan, Italy), BPTES, Etomoxir, CB839, V9302 and IACS-10759 were purchased from Selleck Chemicals (Houston, TX, USA). Stock concentrations were prepared in DMSO (Sigma Aldrich, St Louis, MO, USA) and aliquoted to reduce the thawing-freezing cycle. Final DMSO concentration in medium never exceeded 0.1 %.

2.3. Glucose uptake and consumption

Evaluation of glucose uptake was conducted using the Deoxy-D-glucose-2-[1,2-3H(N)] (2DG, PerkinElmer, Waltham, MA, USA) as previously described [27] and expressed as pmol of 2DG/mg protein/5 min.

Glucose in the medium was estimated using the Glucose (HK) Assay Kit (Sigma-Aldrich) in accordance with the manufacturer's instructions. Glucose consumption values were expressed as μg/ml or as percentage of glucose consumed versus glucose at T_0.

2.4. Lactate production

Lactate in the medium was determined spectrophotometrically by enzymatic assay (Sigma-Aldrich) according to manufacturer's instructions. Lactate production was expressed as μg/ml.

2.5. Glutamine uptake and consumption

Glutamine uptake was conducted as described for glucose using radiolabeled glutamine with some modifications. Cells were seeded in a 12-well plate at a density of 10–12 x 10^4 cells/well. Then, cells were subjected to different treatments for 24 h, washed once with 1 mL of Earle reagent containing 0.25 % of bovine serum albumin for 10 min, then Earle containing 1 μCi/ml radiolabeled glutamine (PerkinElmer) was added to the cell layer and incubated for 1 min. Radiolabeled glutamine taken up by cells was extracted by trichloroacetic acid (5 %). Radioactivity was measured by liquid scintillation. Glutamine uptake values were expressed as pmol/mg protein/min.

Glutamine in the medium was estimated using the bioluminescent Glutamine/Glutamate-Glo™ Assay kit following manufacturer's protocol (Promega, Madison, WI, USA). Glutamine levels were calculated by

subtracting the glutamate-only signal from the total glutamine plus glutamate signal and expressed as percentage of glutamine consumed versus T_0.

2.6. Flow cytometry analysis

For the determination of GLUT1 membrane expression, Alexa Fluor® 488-conjugated antibody (R&D System Minneapolis, MN, USA) was used following the protocol described by Mamun et al. [28]. Data acquisition was performed using a Cytoflex flow cytometer (Beckman Coulter, Brea, CA, USA).

2.7. Cell proliferation and cell death analysis

Cell proliferation/viability of cells was evaluated using either tetrazolium dye [3-(4,5-dimethylthiazol- 2-yl)-2,5-diphenyltetrazolium bromide] (MTT) or Crystal Violet (CV) (triphenylmethane dye (4-[(4-dimethylaminophenyl)-phenyl-methyl]- N, N-dimethyl-aniline) assays as previously described [29]. Color absorbance was measured at 565 nm, or 570 nm for MTT or CV, respectively, using the Infinite 200 PRO microplate reader (Tecan, Männedorf, Switzerland). Cell death was assessed using the fluorescence microscope after Hoechst 333,342 and propidium iodide staining as previously described [30].

The nature of interaction between UK5099 and CB839 was calculated using the Bliss additivism model as previously described [31].

2.8. Western blot analysis

Procedures for protein extraction and analysis by 1D PAGE are described elsewhere [24]. Antibodies against pEGFR^{tyr1068}, EGFR, p-AKT^{ser473}, p-AKT^{thr308}, AKT, p-ERK1/2, ERK1/2, p-AMPK, AMPK, ASCT2, actin, and HRP-conjugated secondary antibodies were from Cell Signaling Technology (Danvers, MA, USA), the chemiluminescence system (Immobilion^{TM} Western Chemiluminescent HRP Substrate) was from Millipore (Temecula, CA, USA). Reagents for electrophoresis and blotting analysis were from BIO-RAD (Hercules, CA, USA). C-DiGit®, LI-COR Blot Scanner was used to acquire the chemiluminescent signal and quantitative analysis was performed by Image Studio^{TM} Software, LI-COR Biotechnology (Lincoln, NE, USA).

2.9. OCR measurement

The oxygen consumption rate (OCR) was measured by a Seahorse Extracellular Flux XFp analyzer (Seahorse Bioscience, North Billerica, MA, USA) according to the manufacturer's instructions. The evaluation of the specific mitochondrial substrates that are required for cellular function was conducted using the Agilent Seahorse XF Substrate Oxidation stress. The Oxidation Stress test combines the substrate pathway-specific inhibitors such as Etomoxir which inhibits Long-Chain Fatty Acids (LCFAs) oxidation through inhibition of carnitine palmitoyl transferase 1a, BPTES for inhibition of glutamine through GLS-1 inhibition and UK5099 for glucose and/or pyruvate through inhibition of the mitochondrial pyruvate carrier (MPC). The maximal respiration and the ATP production were calculated as previously described [27] and the OCR, calculated as pmol/min and normalized to the μg of proteins of each condition, was expressed as percentage of control.

2.10. Intracellular content of lactate, glutamate, and succinate measurement

PC9BRAFG469A cells, plated at 4 x 10^5 cells/dish (25 cm2) density, were incubated for 24 h in the presence of 5 mM (control condition, ctrl) or 1 mM glucose. Five independent wells were harvested for each condition. After incubation, cells were treated with absolute EtOH (1.2 mL, 4 °C) to extract intracellular content. Cell extracts were centrifuged (10000 g, 5 min, 4 °C) and the supernatants were collected. Cell proteins were quantified after solubilization of the cell pellet in NaOH 0.5 N (2 mL/25 cm^2 dish) by the Bradford method. Lactate, glutamate, and succinate were dosed in cell extracts by liquid chromatography-high resolution mass spectrometry (LC-HRMS) employing the standard addition method procedure. Briefly, 100 μL aliquots of cell extract were dried under nitrogen stream and reconstituted into 100 μL of ultra-pure water. Reconstituted extracts were centrifuged (13000 g, 10 min, 4 °C) and 90 μL of supernatant were taken and diluted 1:1 with standard solutions of target analytes to obtain final concentrations of 0.05, 0.15, 0.5, 1.5, 3 and 6 μM in the case of lactate 0.1, 0.3, 1 and 3 μM in the case of glutamate and 0.05, 0.15, 0.5 and 1.5 μM for succinate. An additional aliquot was used as non-spiked sample. A Thermo Vanquish Flex UHPLC system, equipped with a Waters Acquity HSS T3 UPLC column (2.1 x 100 mm; 1.8 μm particle size), thermostated at 45 °C was used for chromatographic separation under isocratic conditions (99 %A; 1 %B). Eluent A: ultra-pure water + 0.1 % formic acid; eluent B: LC-MS grade MeCN + 0.1 % formic acid. Flow rate: 0.3 mL min − 1.

A Thermo Orbitrap Exploris 120, operating in negative ion mode and in full scan acquisition (m/z: 50–300) with a resolution of the Orbitrap analyzer of 60,000 was used for LC-HRMS analysis. Each cell extract was analyzed in four technical replicates and all the samples were randomized prior to analysis. For quantitative analysis, the accurate masses of each analyte were monitored as their [M−H]- ions; lactate: m/z = 89.0244; glutamate: m/z = 146.0459; succinate: m/z = 117.0193. Errors in mass attribution were always lower than 3 ppm. Standard addition regression curves showed good linearity with determination coefficients (r2) > 0.94 for lactate, > 0.93 for glutamate and > 0.99 for succinate. Levels are expressed as nmol/mg of protein.

2.11. Statistical analysis

Quantitative data are mean ± standard deviation (SD) of at least 3 independent determinations. GraphPad Prism version 8.0 software (GraphPad Software Inc., San Diego, CA, USA) was used for data analysis. Differences between the mean values recorded for different experimental conditions were evaluated by Student's *t*-test or by one-way ANOVA and P values are indicated where appropriate in the figures. P values equal to or less than 0.05 were considered statistically significant.

3. Results

3.1. Osimertinib inhibited glucose consumption in osimertinib-sensitive and -resistant cells with EGFR-independent mechanisms of resistance

To investigate the role of metabolic reprogramming in sustaining resistance to osimertinib, we firstly analyzed the effect of osimertinib on glucose consumption and lactate production in PC9 and PC9T790M osimertinib-sensitive cells (IC_{50} for osimertinib determined after 72 h of treatment of 14.4 ± 2.3 and 7.6 ± 0.5 nM, respectively), in PC9BRAFG469A (the resistant clone derived from PC9 cells), and in PC9T790MclA, and PC9T790MC797S (derived from PC9T790M cells). All resistant cells showed osimertinib IC_{50} > 1000 nM. The origin and characteristics of the resistant clones were described in the Materials and methods section. All resistant clones were always grown in the presence of a final concentration of 500 nM osimertinib in the culture medium.

Osimertinib reduced glucose consumption in the osimertinib-sensitive PC9 and PC9T790M cells (Fig. 1A-B). Moreover, osimertinib reduced glucose consumption in resistant clones with EGFR-independent mechanisms of resistance, i.e. PC9BRAFG469A and PC9T790MclA (Fig. 1A-B), while the resistant clone with an EGFR-dependent mechanism of resistance, PC9T790MC797S, retained the ability to utilize glucose in presence of osimertinib (Fig. 1B).

To further confirm these data, we measured lactate production. As shown in Fig. 1C-D, lactate production was found to be reduced in

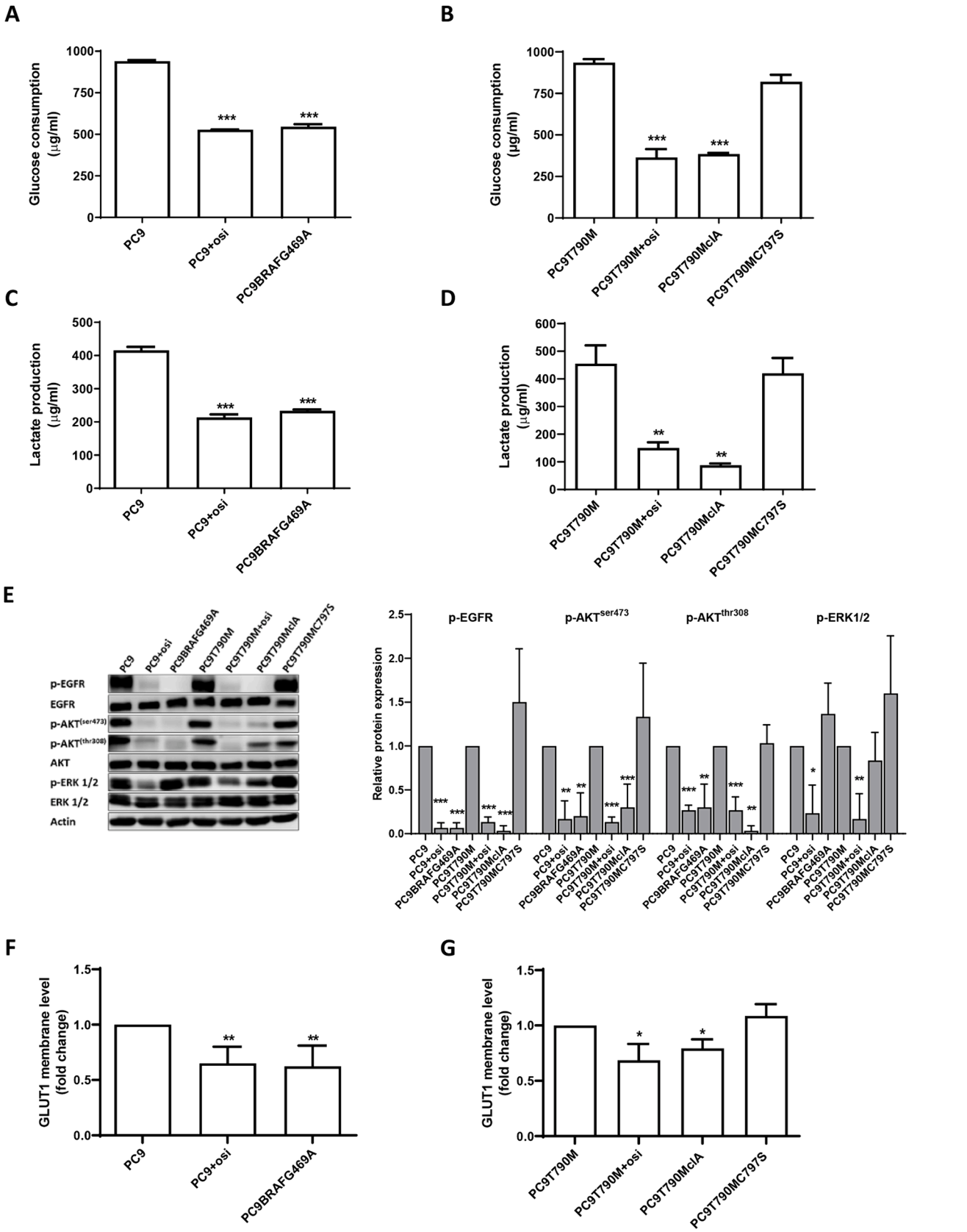

(caption on next page)

Fig. 1. Effects of osimertinib treatment on glucose consumption, lactate production, and signaling pathways in osimertinib-sensitive and resistant cells. PC9 and PC9T790M sensitive cells were cultured in absence or in presence of 100 nM osimertinib, PC9BRAFG469A, PC9T790MclA and PC9T790MC797S resistant clones were cultured with 500 nM osimertinib. After 24 h, glucose consumption (A-B) and lactate production (C-D) were assessed as described in Material and methods section. (E) Western Blotting analysis was performed to evaluate the phosphorylation/expression of the indicated proteins; quantitative analyses derived from three western blotting experiments; the ratios between each phosphoprotein and the corresponding total protein were calculated, and the data are expressed as fold increase *vs* the corresponding untreated osimertinib-sensitive cells; the analysis of the different proteins are from blots cut prior to hybridization with different antibodies for the phosphorylated forms or from membrane after stripping for detecting total proteins. (F) Membrane GLUT1 expression in PC9 and PC9BRAFG469A was analyzed by flow cytometry and expressed as fold change *vs* untreated PC9 cells. (G) Membrane GLUT1 expression in PC9T790M and PC9T790MclA and PC9T790MC797S was analyzed by flow cytometry and expressed as fold change *vs* untreated PC9T790M cells.* $p < 0.05$, ** $p < 0.01$, *** $p < 0.001$ *vs* untreated osimertinib-sensitive cells.

osimertinib-sensitive cells, PC9, and in the osimertinib-resistant clone PC9BRAFG469A; the same results were obtained in osimertinib-sensitive cells PC9T790M and in the osimertinib-resistant clone PC9T790MclA; however, PC9T790MC797S cells were similar to the parental cell line regarding lactate production.

To further explain the mechanism behind the reduction of glucose consumption, we analyzed the signaling pathways affected by osimertinib and, as shown in Fig. 1E, the ability of osimertinib to inhibit EGFR and downstream AKT phosphorylation in sensitive cells and resistant clones bearing EGFR-independent mechanisms of resistance may influence the expression of glucose transporters on the plasma membrane as confirmed by the flow cytometry analysis shown in Fig. 1F-G. A decreased GLUT1 expression was observed in PC9 and PC9T790M treated with osimertinib and in the resistant clones PC9BRAFG469A and PC9T790MclA, but not in PC9T790MC797S.

3.2. Effect of inhibition of glutamine, pyruvate, and fatty acid oxidation on mitochondrial respiration and ATP production in osimertinib-resistant cells

Considering that, despite low glucose consumption, resistant clones were able to survive and proliferate in the presence of 500 nM osimertinib, we evaluated, by Agilent Seahorse XF, the role of the primary substrates glucose/pyruvate, glutamine, and LCFAs in driving mitochondrial function. To this end, we performed acute injections of assay media (ctrl), BPTES (for inhibition of glutamine through the inhibition of GLS1), UK5099 (for inhibition of glucose/ pyruvate through the inhibition of MPC) or etomoxir (for inhibition of LCFAs through the inhibition of carnitine palmitoyl transferase 1a) followed by the sequential injections of oligomycin, Carbonyl cyanide-p-trifluoromethoxyphenylhydrazone FCCP, and rotenone/antimycin. As shown in Fig. 2A-B, a significant inhibition of the maximal respiration was observed with BPTES in both PC9BRAFG469A and PC9T790MclA

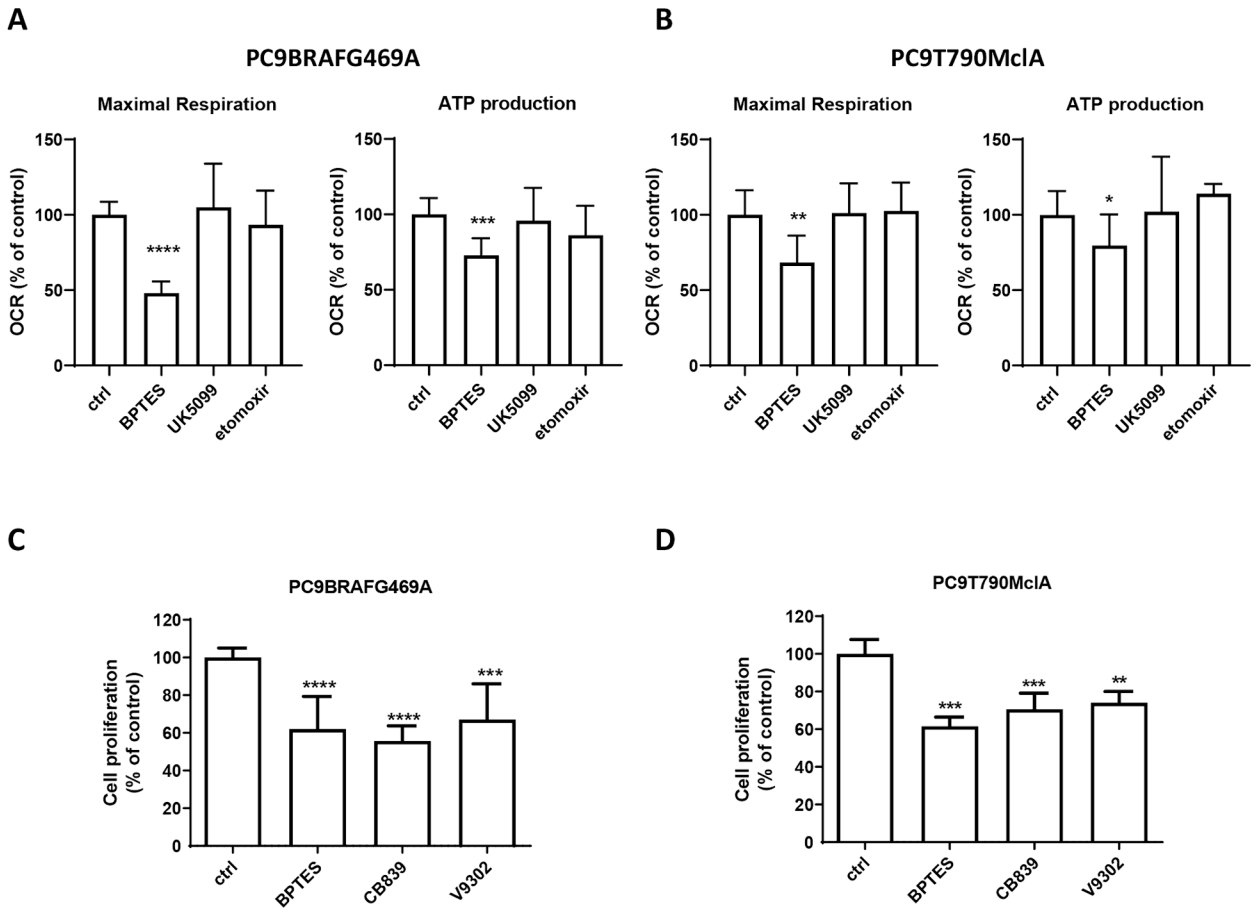

Fig. 2. Effects of inhibition of mitochondrial substrates on mitochondrial respiration in PC9BRAFG469A and PC9T790MclA osimertinib-resistant cells. Mitochondrial respiration was analyzed by the Agilent Seahorse XF Substrate Oxidation Stress Test as described in Material and methods section. The parameters of maximal mitochondrial respiration and ATP production (A-B) were calculated. (C-D) Cell proliferation was assessed by crystal violet assay in cell clones treated for 48 h with BPTES (10 μM), CB839 (10 μM), and V9302 (10 μM). * $p < 0.05$, ** $p < 0.01$, *** $p < 0.001$, **** $p < 0.0001$ *vs* untreated cells (ctrl).

cell clones, while no effect was seen with etomoxir and UK5099. Accordingly, a significant decrease in the respiration associated with ATP production was observed only with BPTES (Fig. 2A-B). These data suggest a greater dependence on glutamine than glucose or fatty acids for oxygen consumption and energy production in both cell clones.

To further evaluate and confirm the dependence on glutamine in the resistant clones, we assessed cell proliferation upon inhibition of either glutamine uptake, using the ASCT2 inhibitor V9302, or glutamine conversion to glutamate, using BPTES or CB839 (a GLS1 inhibitor under clinical trial for NSCLC patients in combination with osimertinib, NCT03831932). Inhibition of glutamine metabolism by all these inhibitors significantly reduced cell proliferation in both resistant clones (Fig. 2C-D).

3.3. Osimertinib-resistant cells with EGFR-independent mechanisms of resistance survived and proliferated under glucose starvation

Since resistant clones with EGFR-independent mechanisms of resistance take up and consume low glucose, as described above, we determined the minimum glucose levels required for sustaining cell viability by evaluating the effect of glucose starvation on cell proliferation and death. We found that PC9BRAFG469A resistant cells were able to proliferate and survive at 1 mM of glucose, unlike their parental cell line PC9, which failed to proliferate (Fig. 3A) and survive (Fig. 3B) at the same concentration of glucose. Similar results were observed in PC9T790MclA cells compared to parental PC9T790M cells (Fig. 3C-D); by contrast, the EGFR-dependent resistant clone PC9T790MC797S was markedly sensitive to glucose starvation and failed to proliferate even at 2.5 mM of glucose (Fig. 3C), reflecting its high dependence on glucose.

3.4. Glucose starvation enhanced glucose and glutamine uptake and consumption in osimertinib-resistant cells

Then, we evaluated how resistant cells developed the ability to survive under low glucose environment. Firstly, we evaluated glucose uptake and consumption at 5 mM (hereafter defined as control) and 1 mM glucose after 24 h. As shown in Fig. 4A-B, glucose uptake increased greatly at 1 mM compared to control in both PC9BRAFG469A and PC9T790MclA cells and was accompanied by an increase in the glucose consumption (Fig. 4C-D). We then analyzed the signaling pathways involved in survival under low-nutrient conditions and found an increase in the phosphorylation of the enzyme 5′ Adenosine Monophosphate-activated Protein Kinase (AMPK) at 1 mM glucose compared to 5 mM through time (8, 16, 24 and 48 h, Fig. 4E). Since AMPK activation increases glucose uptake under low energy conditions [32], we evaluated glucose uptake at 1 mM glucose in PC9BRAFG469A cells at 4, 8, and 16 h. Glucose uptake significantly increased through time at 1 mM compared with the control (Fig. 4F).

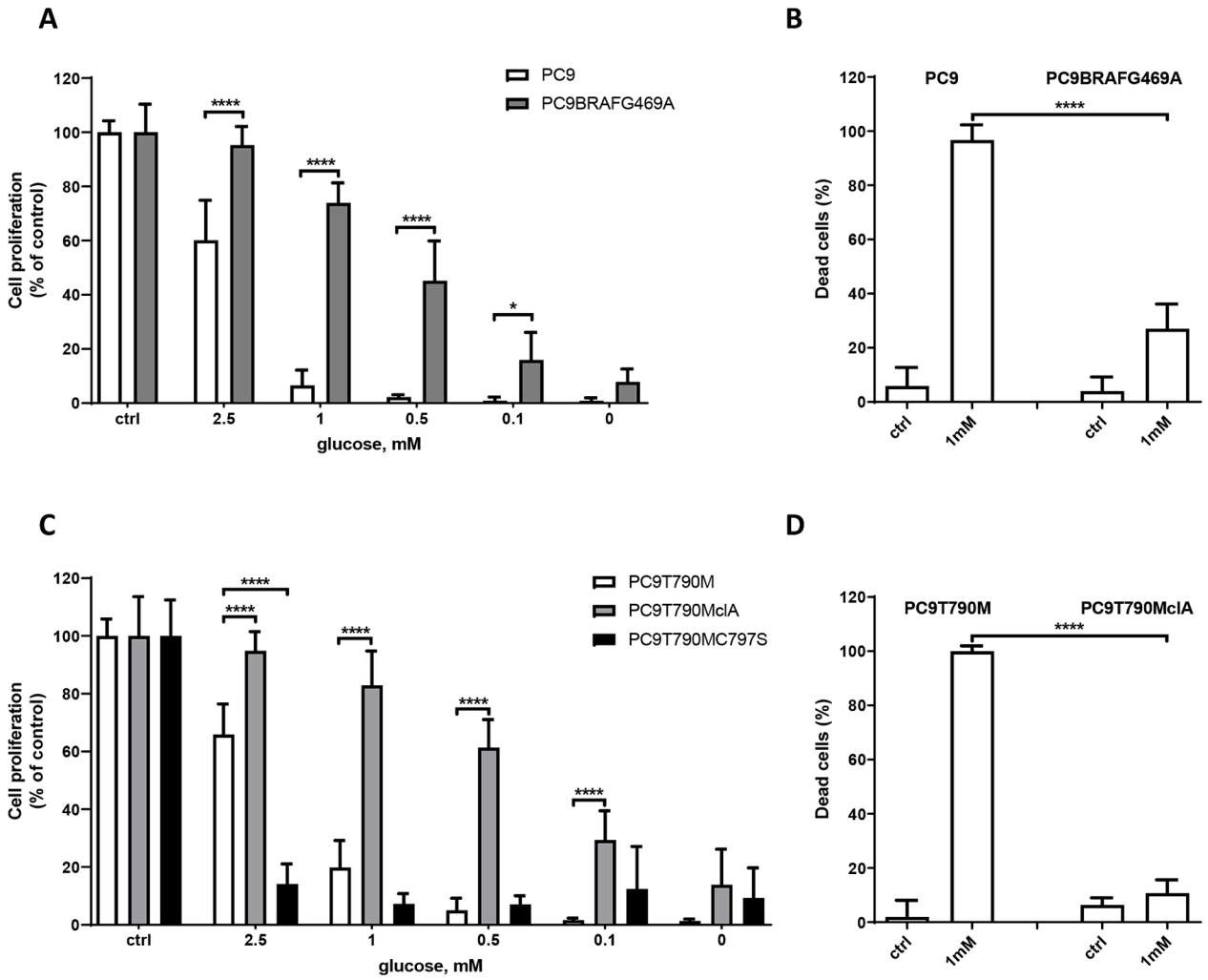

Fig. 3. Effects of glucose starvation on cell proliferation and cell death in osimertinib-sensitive cells and resistant clones. The indicated cells were cultured with different concentrations of glucose in the culture medium. After 48 h, cell proliferation (A-C) and cell death (B-D) were analyzed by crystal violet assay and by fluorescence microscopy after Hoechst 33342/PI staining, respectively. * $p < 0.05$, **** $p < 0.0001$ *vs* osimertinib-sensitive parental cells.

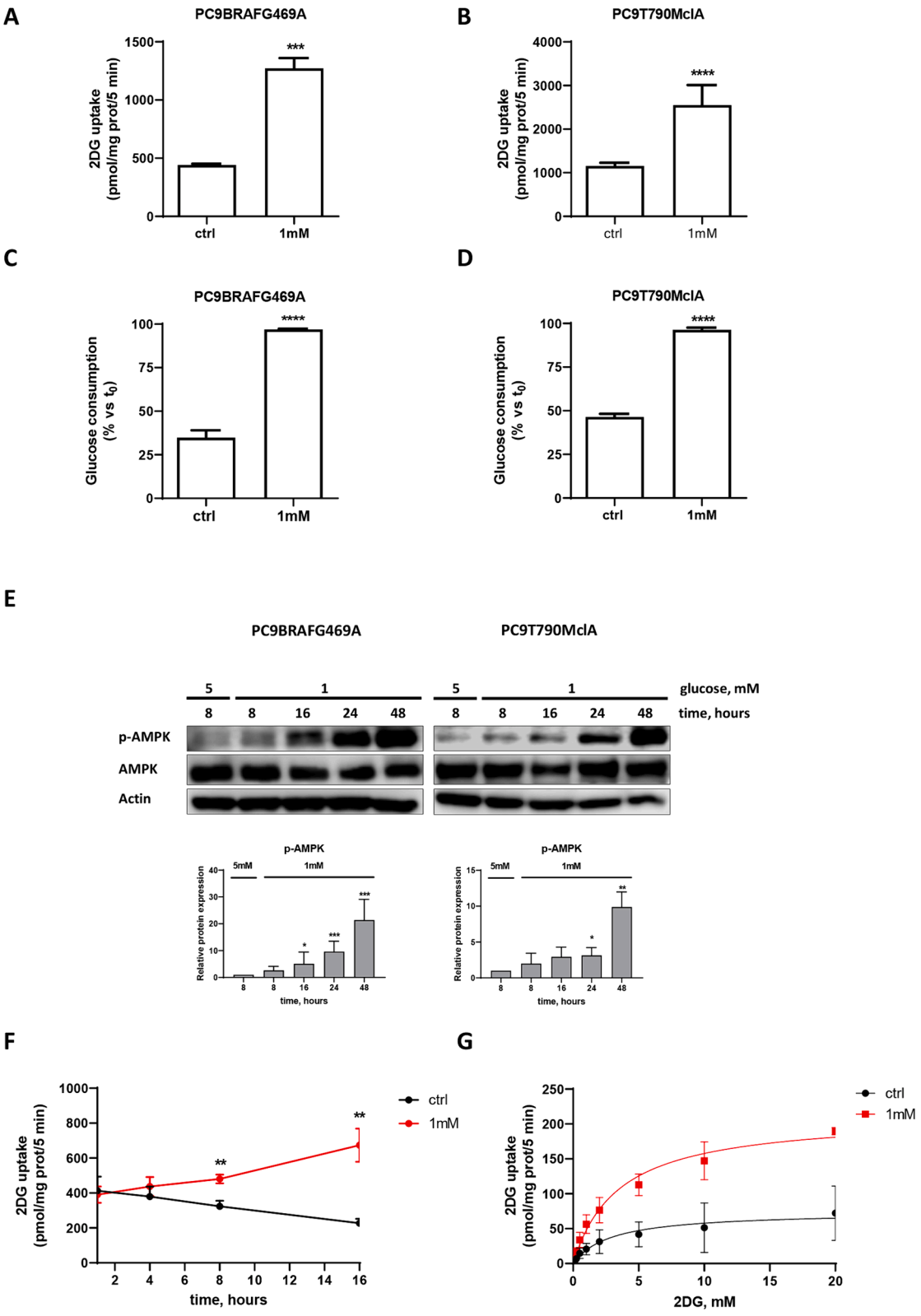

Fig. 4. Effects of glucose starvation on glucose uptake and consumption in PC9BRAFG469A and PC9T790MclA osimertinib-resistant cells. PC9BRAFG469A PC9T790MclA cells were cultured with 5 mM (crtl) or 1 mM glucose; glucose uptake (A-B) and glucose consumption (C-D) were assessed after 24 h. (E) Western blot analysis was performed at 8, 16, and 24 h to evaluate the phosphorylation of AMPK; quantitative analyses derived from three Western blotting experiments; the ratios between each phosphoprotein and the corresponding total protein were calculated, and the data are expressed as fold increase *vs* 5 mM glucose; (F) PC9BRAFG469A cells were cultured in control condition (ctrl) or 1 mM glucose, then glucose uptake was measured after 4, 8, and 16 h; (G) Kinetics of glucose uptake at normal (ctrl) and low glucose (1 mM) in PC9BRAFG469A. ** $p < 0.01$, *** $p < 0.001$, **** $p < 0.0001$ *vs* ctrl.

The increased glucose uptake in PC9BRAFG469A cells was confirmed by evaluating the kinetics of glucose transport (Fig. 4G). The initial velocity of 2DG transport as a function of substrate concentrations was measured in cells incubated at 5 mM (control) or 1 mM glucose over a broad range of substrate concentrations. For control cells, after 16 h of incubation, the best fit equation corresponded to values of 2.876 mM for Km (95 % CI: 1.158 to 7.894) and 74.38 pmol/mg protein/5min of 2DG for Vmax (95 % CI: 54.80 to 107.7). For cells incubated at 1 mM glucose for 16 h, the corresponding values were 3.468 mM for Km (95 % CI: 2.607 to 4.663) and 212.4 pmol/mg protein/5min of 2DG for Vmax (95 % CI: 193.2 to 234.9). Taken together, these results suggest that the affinity of 2DG transporter increases slightly but the capacity of the system of mediation increases several times under glucose starvation.

We also evaluated the effect of glucose starvation on glutamine uptake and consumption. In PC9BRAFG469A cells, glucose starvation (1 mM) resulted in a significant enhancement of glutamine uptake and consumption compared to the condition of control glucose level (Fig. 5A-B). In contrast, in PC9T790MclA cells, glutamine uptake remained unchanged at 1 mM glucose with no statistical difference in its consumption (Fig. 5C-D). The increase of glutamine uptake in a low glucose environment in PC9BRAFG469A cells was attributed to the increased expression of the glutamine transporter ASCT2 compared to 5 mM glucose. The unchanged glutamine uptake in PC9T790MclA cells under glucose starvation could be due to the higher basal level of ASCT2 expression, which remained unaffected (Fig. 5E) and could also explain the higher glutamine uptake compared to PC9BRAFG469A cells. The high basal ASCT2 expression and the high glutamine uptake observed in normal glucose condition may concur for a better adaptation in low glucose conditions of PC9T790MclA cells.

3.5. *Inhibition of glutamine and pyruvate utilization decreased mitochondrial respiration and ATP production in osimertinib-resistant cells*

Furthermore, we examined the effects of inhibiting mitochondrial glutamine and pyruvate utilization as well as fatty acid oxidation on mitochondrial respiration and ATP production under glucose starvation in the resistant clones. We demonstrated that either inhibiting glutamine utilization by BPTES or inhibiting pyruvate transport into mitochondria using UK5099 led to a significant decrease in mitochondrial maximal respiration and ATP-linked respiration in PC9BRAFG469A and PC9T790MclA cells. By contrast, inhibition of fatty acid oxidation using etomoxir affected neither maximal respiration nor ATP production in both resistant clones, suggesting that cell respiration did not rely on fatty acid oxidation under glucose starvation conditions (Fig. 6A-B).

Then, we measured the production of lactate at 5 (control) and 1 mM glucose and observed a strong reduction in the lactate production at 1 mM in both resistant clones (Fig. 6C), suggesting an increased transport of pyruvate into mitochondria to supply increased mitochondrial

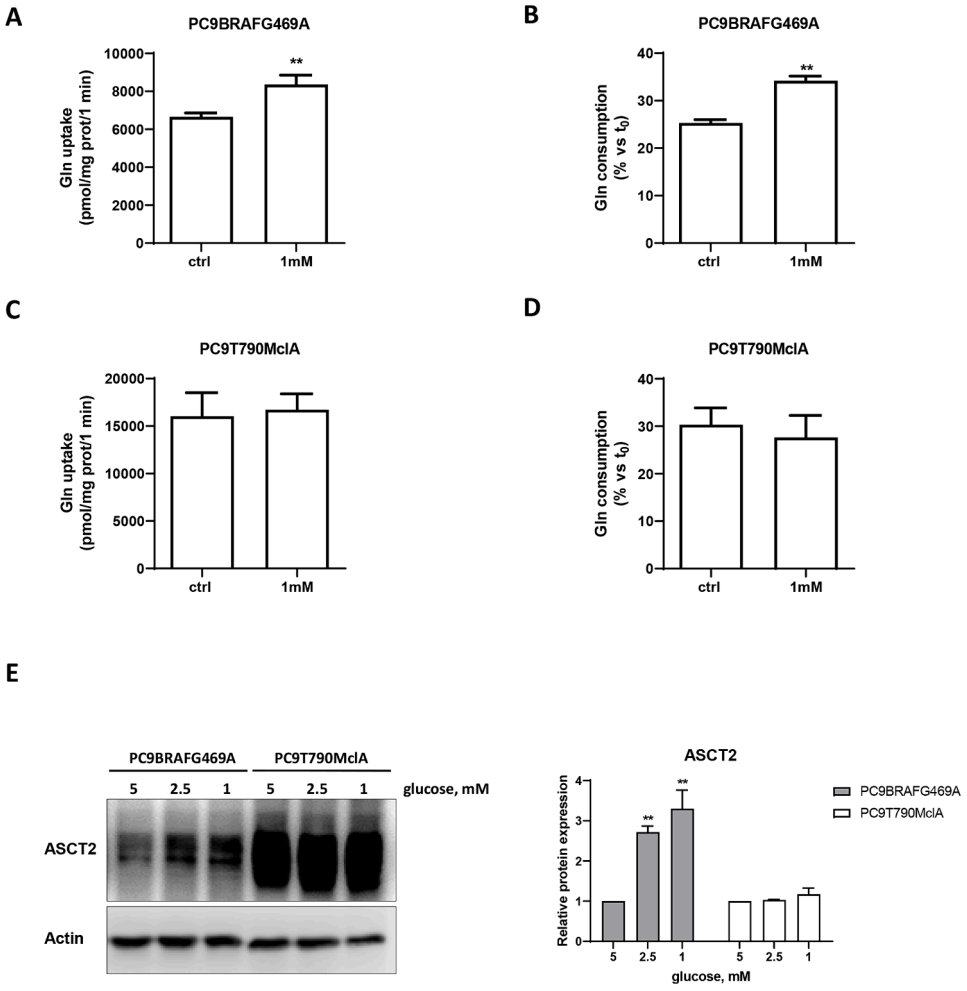

Fig. 5. Effects of glucose starvation on glutamine uptake and consumption, and glutamine transporter expression in PC9BRAFG469A and PC9T790MclA cells. Glutamine uptake (A-C) and glutamine consumption (B-D) were measured after 24 h of glucose starvation (1 mM) compared to control glucose levels (ctrl) in PC9BRAFG469A and PC9T790MclA cells; (E) PC9BRAFG469A and PC9T790MclA cells were cultured with 5, 2.5 and 1 mM for 24 h, then Western Blot analysis was performed to evaluate the expression of the glutamine transporter ASCT2; quantitative analyses derived from three Western Blot experiments; the ratios between ASCT2 protein and actin were calculated, and data for each cell model are expressed as fold increase *vs* the corresponding 5 mM glucose condition. ** $p < 0.01$ *vs* ctrl.

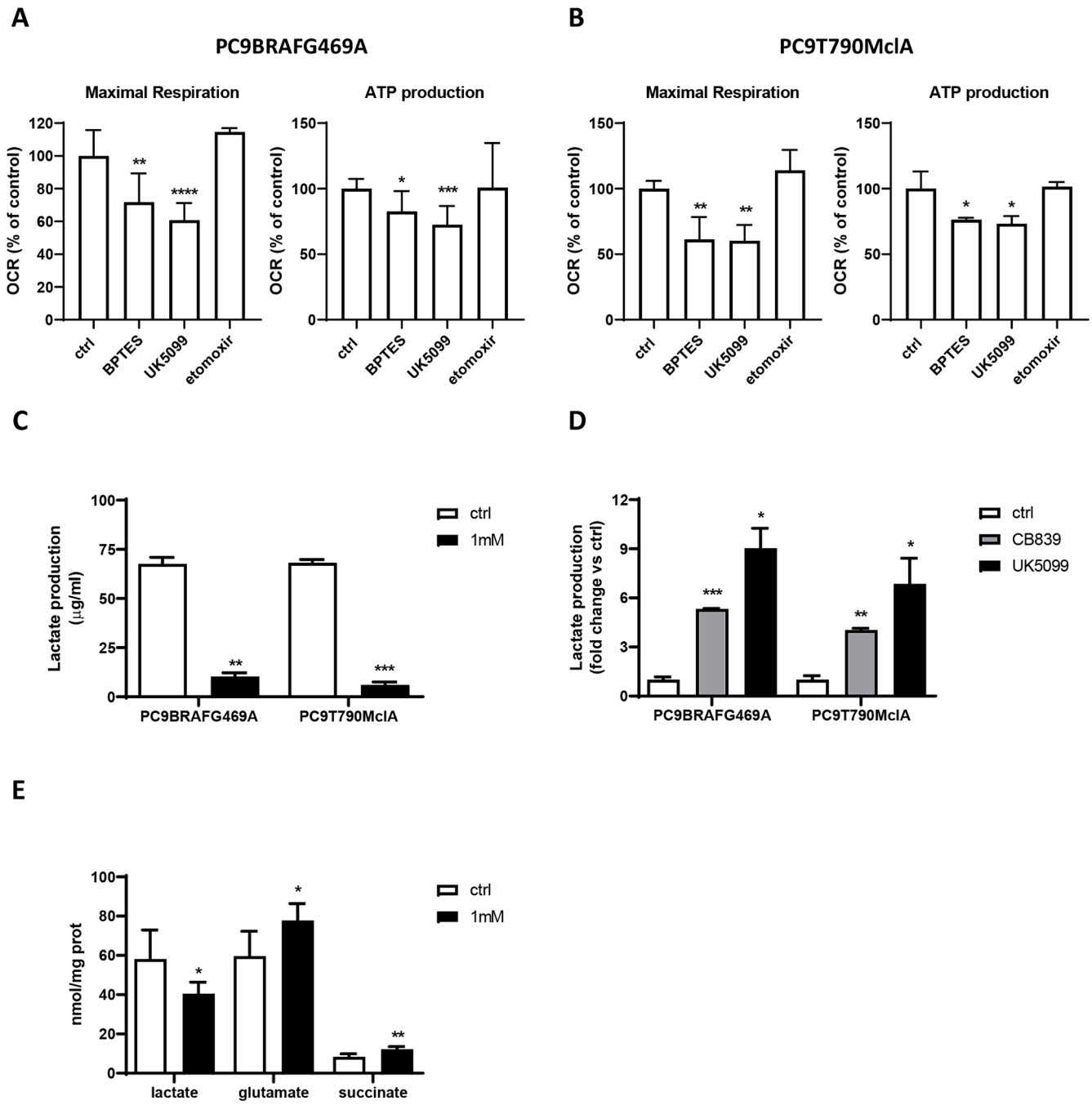

Fig. 6. Effects of inhibition of glutamine, pyruvate, and fatty acid utilization in the mitochondria on mitochondrial respiration, ATP, and lactate production in PC9BRAFG469A and PC9T790MclA cells under glucose starvation. (A-B) Mitochondrial respiration was analyzed by the Agilent Seahorse XF Substrate Oxidation stress. Parameters of maximal mitochondrial respiration and ATP production were calculated. (C) PC9BRAFG469A and PC9T790MclA cells were cultured in control condition (ctrl) or at 1 mM glucose for 24 h then lactate production was determined. (D) PC9BRAFG469A and PC9T790MclA cells were treated with 10 μM CB839 or 10 μM UK5099 for 48 h in control condition (ctrl) or at 1 mM glucose, then lactate production was determined. (E) Intracellular glutamate, succinate, and lactate levels in PC9BRAFG469A cell line cultured in control condition (ctrl) or at 1 mM glucose for 24 h. A, B, D: * $p < 0.05$, ** $p < 0.01$, *** $p < 0.001$, **** $p < 0.0001$ *vs* untreated cells (ctrl); C, E: * $p < 0.05$, ** $p < 0.01$, *** $p < 0.001$ *vs* ctrl.

activity, rather than a reduction to lactate. Moreover, we observed a significant increase in lactate production when we inhibited glutamine utilization and pyruvate transport into mitochondria using CB839 and UK5099, respectively (Fig. 6D), indicating a shift to glycolysis and a decrease in mitochondrial metabolism.

To further confirm the increased dependence on mitochondrial metabolism under low glucose environment, we analyzed and measured the intracellular levels of different mitochondrial substrates supplied by glycolytic and glutamine intermediates using LC-MS. These metabolites include lactate, glutamate as well as Kreb's cycle metabolite succinate. We found that at 1 mM glucose, intracellular levels of glutamate and succinate were significantly higher compared to the condition of control glucose level (Fig. 6E), explaining the increased glutamine uptake and increased mitochondrial function, respectively, under low glucose. The levels of lactate were significantly lower at 1 mM compared to control condition, reflecting the increased transport of pyruvate inside mitochondria rather than the reduction to lactate in cells grown in a low glucose environment.

3.6. Hindering mitochondrial glutamine and pyruvate utilization inhibited cell proliferation and cell survival of osimertinib-resistant clones

To further evaluate the role of mitochondrial metabolism in resistant clones under glucose starvation, we evaluated the effects of inhibiting glutamine and pyruvate mitochondrial utilization on cell proliferation and survival. As shown in Fig. 7A-D, PC9BRAFG469A and PC9T790MclA cells under low glucose conditions were more sensitive to the treatment with CB839 and UK5099 than in the control condition. In addition, we evaluated cell proliferation upon inhibition of OXPHOS using the complex I inhibitor IACS in PC9BRAFG469A and PC9T790MclA cells. We found that OXPHOS inhibition, inhibited cell proliferation at 1 mM glucose but no relevant inhibition was observed in the control condition in both resistant clones (Fig. 7E-F). We then evaluated cell death upon treatment with CB839, UK5099, and IACS at 5 and 1 mM of glucose. As shown in Fig. 7G-H, a significant cell death at 1 mM of glucose was observed in PC9BRAFG469A and PC9T790MclA when compared to the condition of control glucose level.

Finally, we sought to elucidate the effects of combinations of pyruvate transport inhibition and glutamine utilisation suppression in low-glucose environment on the inhibition of cell proliferation in PC9T790MclA cells. To this aim we treated the cells with increasing concentrations of UK5099 with a fixed concentration of CB839 (10 μM) for 48 h and using the Bliss additivism model, we observed a synergistic inhibition of cell proliferation (Fig. 7I).

This, along with the previous data on glucose and glutamine uptake and consumption, as well as the reduced cell proliferation and survival upon inhibition of GLS1, MPC, and OXPHOS at 1 mM of glucose, confirms the increased dependence on mitochondrial metabolism in low glucose environment. Altogether, these results confirm the enhanced mitochondrial metabolism under glucose starvation, which depends on the use of pyruvate and glutamate rather than fatty acids.

4. Discussion

Reprogramming the metabolic profile is one of the hallmarks of cancer. Among mutations of oncogenes and tumor suppressor genes that lead to the gain or loss of functions, respectively, there are some alterations that reprogram the metabolic profiles of cancer cells, enabling rapid division, proliferation, survival, and the promotion or maintenance of drug resistance. These alterations lead to the inhibition or activation of signaling pathways and transcriptional networks involved in the metabolism of carbohydrates, lipids, and proteins. These adaptations are important for energy production to balance energy status inside tumour cells, the production of synthetic molecules needed for growth and the synthesis of molecules required for redox balance maintenance.

Among the mutations associated with the development of NSCLC there are the activating *EGFR* mutations targeted by TKIs as the first line treatment [33]. Osimertinib represents the last EGFR TKI mutant selective entered in clinical practice and approved for all *EGFR*-mutated patients.

The aim of this study was to analyse the role of metabolic reprogramming in sustaining osimertinib-resistance in NSCLC *EGFR*-mutated cell lines in low glucose environment and to find vulnerable metabolic pathways to target.

Firstly, we demonstrated that osimertinib-sensitive *EGFR*-mutated NSCLC cell lines exhibit decreased glucose consumption and reduced lactate production when treated with osimertinib. These observations are consistent with previous results by Makinoshima et al., who reported a decreased expression of both GLUT1 and GLUT3 upon inhibition of EGFR using erlotinib in lung adenocarcinoma cell lines, leading to decreased glycolytic activity [9]. In our resistant models with EGFR-independent mechanisms of resistance as well as in sensitive cells, the reduction in glucose consumption can be attributed to the inhibition of the AKT pathway, highlighting the well-known role of AKT signaling in regulating glucose uptake by stimulating the translocation of GLUT1 to the cell membrane [34].

We observed distinct metabolic profiles and responses to metabolic perturbations between EGFR-dependent and EGFR-independent resistant cells. Specifically, EGFR-dependent cells exhibited an energetic phenotype characterized by a significant reliance on glycolysis and mitochondrial metabolism. This heightened metabolic activity was evidenced by their equal consumption of glucose and production of lactate compared to their control parental cell line. Moreover, our results demonstrate that EGFR-dependent cells displayed high sensitivity to glucose deprivation, even greater than their parental cell line. This heightened sensitivity to glucose deprivation highlights the critical role of glycolysis in sustaining the energetic demands of EGFR-dependent resistant cells.

In contrast, EGFR-independent resistant clones exhibited metabolic adaptations that enabled survival under glucose deprivation conditions. These clones displayed altered metabolic dependencies and strategies to circumvent glucose scarcity, reflecting their distinct metabolic reprogramming in the context of acquired resistance.

Glutamine serves as a nitrogen source and directly or indirectly participates in numerous cancer-related anabolic processes, including the synthesis of amino acids, nucleobases, and hexosamines. Additionally, it plays a crucial role in maintaining redox balance. Importantly, when converted to α-ketoglutarate, glutamine serves as both an energy source and a mean of replenishing intermediates in the TCA, providing essential carbon for cellular processes [21].

The role of glutamine metabolism in drug resistance has been extensively reviewed [35,36]. In EGFR-TKI resistance, a strong dependence on glutamine has been reported in two acquired EGFR-TKI-resistant lung cancer cell lines (HCC827 gefitinib-resistant and H292 erlotinib- resistant) [37] based on its role in redox balance or as carbon source for TCA-cycle intermediates.

It has been reported that the inhibition of GLS-1 using CB839 led to a potent inhibition of NSCLC cells viability, and the effect of CB839 in vivo was cooperative with erlotinib and induced energetic stress and autophagy [38,39].

In osimertinib-resistant cells a substantial decrease in oxygen consumption rate and mitochondrial ATP levels was observed upon inhibition of glutamine conversion to glutamate using BPTES, while no noticeable effect was observed when pyruvate and fatty acids transport into mitochondria was blocked (by UK5099 or etomoxir, respectively). As a consequence of GLS-1 or ASCT2 inhibition, cellular proliferation of resistant clones was significantly reduced indicating heightened reliance on glutamine for sustaining cellular functions in the presence of osimertinib.

The metabolic flexibility of osimertinib-resistant cells, which allowed them to bypass the restriction induced by low glucose uptake and consumption, prompted us to test the ability of cells to optimize nutrient utilization under low glucose conditions. We found that, differently from osimertinib-sensitive cells, resistant cells were able to proliferate and survive under glucose starvation, a stress condition which may be found in tumor microenvironment due to insufficient neovascularization. In a previous study, it was demonstrated that erlotinib and gefitinib-resistant cell lines had low glucose dependency and were able to proliferate in low-glucose environments compared to their sensitive parental cell lines [37].

Here, we demonstrated that resistant cells were able to activate compensatory mechanisms by increasing the rate of glucose and glutamine uptake. The signaling pathway involves AMPK, a protein activated in many tumour cells during conditions of metabolic stress such as insufficient supply of nutrients [40]. In response to glucose starvation, AMPK promotes the uptake of glucose and the oxidation of lipids to generate energy. Simultaneously, it suppresses energy-consuming processes such as glucose and lipid production, aiming to restore equilibrium in energy levels [32]. Moreover, it has been reported that in cancer cells under glucose starvation AMPK was also able to enhance glutamine

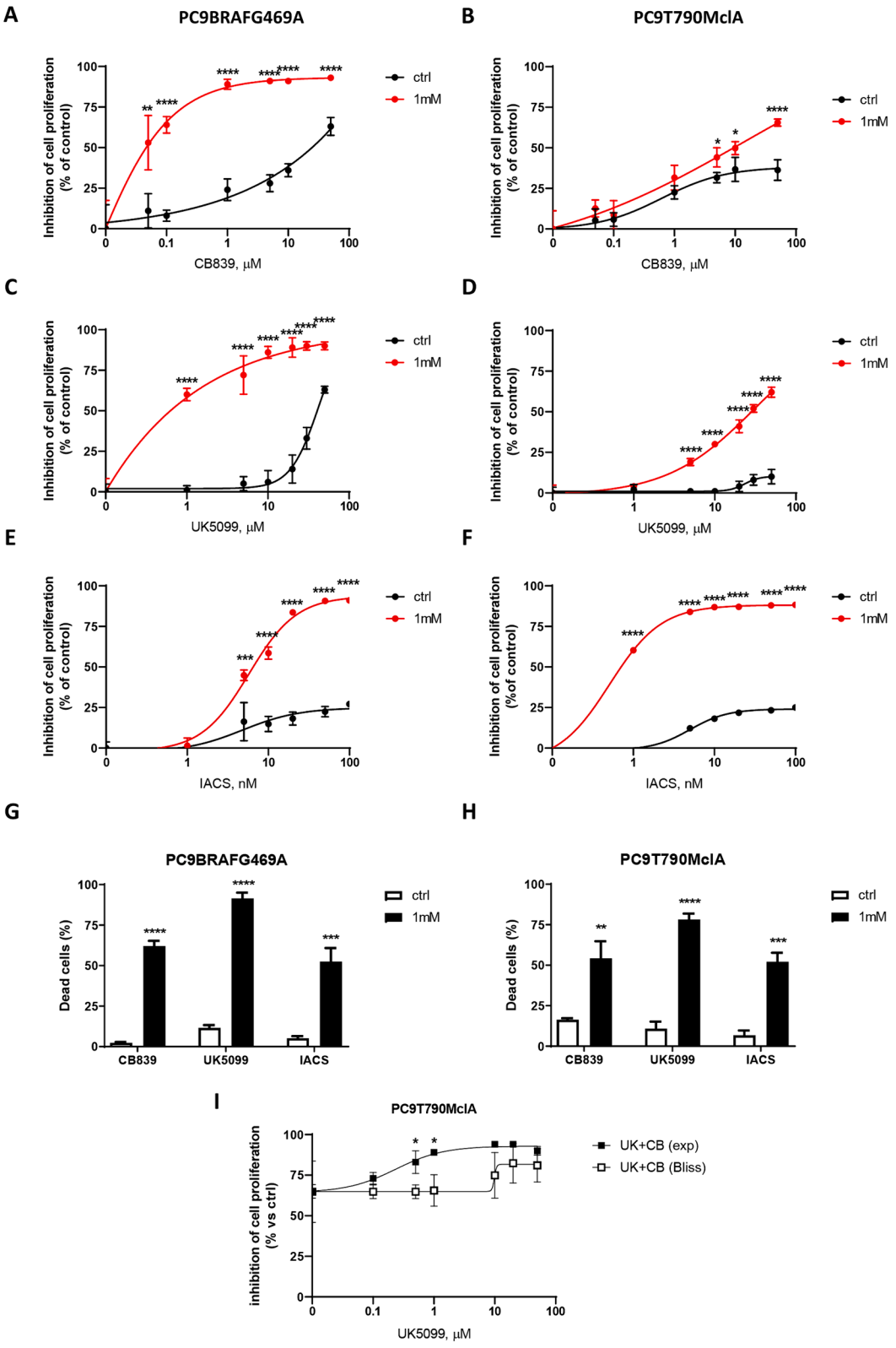

Fig. 7. Effects of inhibition of glutamine and pyruvate utilization and oxidative phosphorylation on cell proliferation in PC9BRAFG469A and PC9T790MclA cells. PC9BRAFG469A and PC9T790MclA cells were treated with increasing concentrations of CB839 (A-B), UK5099 (C-D) or IACS (E-F) for 48 h in normal medium (ctrl) or in low glucose medium (1 mM). Then, the analysis of cell proliferation was evaluated by MTT assay. The data are expressed as percent inhibition *vs* ctrl cells; (G-H) PC9BRAFG469A and PC9T790MclA cells were treated with CB839, UK5099, or IACS for 48 h in control condition (ctrl) or at 1 mM glucose, then cell death was analyzed by fluorescence microscopy after Hoechst 33342/PI staining. * $p < 0.05$, ** $p < 0.01$, *** $p < 0.001$, **** $p < 0.0001$ *vs* ctrl. (I) PC9T790MclA cells were treated with different concentrations of UK5099 in the presence of 10 µM of CB839 in low glucose medium. After 48 h cell proliferation was evaluated by MTT assay. The data are expressed as percent inhibition *vs* ctrl cells and the effect of the drug combination was evaluated using the Bliss interaction model. * $p < 0.05$ *vs* Bliss curve.

uptake through increased expression of ASCT2 [41].

Our results suggest that under limited glucose levels, the resistant cells reprogram their metabolism to support their cellular functions. This reprogramming was evidenced by the inhibition of maximal mitochondrial respiration and ATP production when we hindered the conversion of glutamine to glutamate and the transport of pyruvate to the mitochondria. In contrast, under normal glucose conditions, only the inhibition of glutamine led to a decrease in mitochondrial respiration and ATP production. This indicates that under normal glucose levels, resistant cells are more reliant on glutamine. However, under glucose-starved conditions, they depend on both glutamine and glucose, with no impact of fatty acid oxidation inhibition on mitochondrial respiration and ATP production. Furthermore, inhibition of glutamine and pyruvate utilization for 24 h under glucose-starved conditions increased lactate production. Despite lung cancer cells have the capacity to utilize lactate as a source of fuel in vivo [42], this is not the case for osimertinib-resistant clones, which strongly decreased cell proliferation and cell viability upon inhibition of the utilization of glutamine and pyruvate under low glucose conditions.

In the mitochondria, OXPHOS efficiently produces ATP through the electron carriers NADH and FADH2 derived from the TCA cycle. Glutamine and pyruvate are vital substrates that fuel the TCA cycle. The electrons generated from the oxidation of glutamine and pyruvate, in addition to LCFAs and nucleotides, drive the electron transport chain, resulting in ATP production [43]. Our resistant cells exhibit an increased reliance on OXPHOS fueled by glutamine and pyruvate, rather than LCFAs, as demonstrated by the inhibition of OXPHOS with IACS, which confirm the metabolic reprogramming inside mitochondria under glucose shortage.

In conclusion, our findings demonstrate the remarkable adaptability of osimertinib-resistant NSCLC cells in low glucose environment. These resistant cells exhibited enhanced survival capabilities by enhancing their uptake and utilization of glucose and glutamine. Significantly, our research underscores the pivotal role of mitochondrial metabolism in the resilience of these cells under low glucose conditions. Importantly, targeting the metabolic adaptive responses triggered by glucose shortage emerges as a promising strategy, effectively inhibiting cell proliferation and promoting cell death in osimertinib resistant cells.

CRediT authorship contribution statement

Kamal Eltayeb: Writing – review & editing, Writing – original draft, Investigation, Formal analysis, Data curation, Conceptualization. **Roberta Alfieri:** Investigation. **Claudia Fumarola:** Writing – review & editing, Investigation, Data curation. **Mara Bonelli:** Investigation. **Maricla Galetti:** Validation, Data curation. **Andrea Cavazzoni:** Validation. **Graziana Digiacomo:** Investigation. **Francesca Galvani:** Investigation. **Federica Vacondio:** Investigation. **Alessio Lodola:** Investigation. **Marco Mor:** Writing – review & editing, Supervision. **Roberta Minari:** Investigation. **Marcello Tiseo:** Writing – review & editing, Supervision, Funding acquisition. **Silvia La Monica:** Writing – original draft, Investigation, Formal analysis, Data curation, Conceptualization. **Pier Giorgio Petronini:** Writing – review & editing, Supervision, Investigation, Conceptualization.

Declaration of competing interest

The authors declare that they have no known competing financial interests or personal relationships that could have appeared to influence the work reported in this paper.

Data availability

Data will be made available on request.

Acknowledgements

This research has financially been supported by the Program “FIL-Quota Incentivante” of University of Parma and co-sponsored by Fondazione Cariparma.

The work was also supported by AstraZeneca, Milan, Italy, by AIRC (Italian Association for Cancer Research), Milan, Italy (grant IG2017-20074 PI M. Tiseo) and by Associazione Augusto per la vita, Novellara, RE, Italy. This work has been carried out in the frame of the ALIFAR project, funded by the Italian Ministry of University through the program ‘Dipartimenti di Eccellenza 2023-2027’.

The funders had no role in study design, data collection and analysis, decision to publish, or preparation of the manuscript.

M.T. received speakers’ and consultants’ fee from Astra-Zeneca, Pfizer, Eli-Lilly, BMS, Novartis, Roche, MSD, Boehringer Ingelheim, Otsuka, Takeda, Pierre Fabre, Amgen, Merck, Sanofi. M.T. received institutional research grants from Astra-Zeneca, Boehringer Ingelheim. R.A received institutional research grants from Astra-Zeneca. PGP received institutional research grants from Pfizer and Novartis.

References

[1] H. Sung, J. Ferlay, R.L. Siegel, M. Laversanne, I. Soerjomataram, A. Jemal, F. Bray, Global Cancer Statistics 2020: GLOBOCAN Estimates of Incidence and Mortality Worldwide for 36 Cancers in 185 Countries, CA Cancer J. Clin. 71 (2021) 209–249. Doi: 10.3322/caac.21660.

[2] W.-H. Hsu, J.-C.-H. Yang, T.S. Mok, H.H. Loong, Overview of current systemic management of EGFR-mutant NSCLC, Ann. Oncol. 29 (2018) i3–i9, https://doi.org/10.1093/annonc/mdx702.

[3] J. Hou, H. Li, S. Ma, Z. He, S. Yang, L. Hao, H. Zhou, Z. Zhang, J. Han, L. Wang, Q. Wang, EGFR exon 20 insertion mutations in advanced non-small-cell lung cancer: current status and perspectives, Biomark Res. 10 (2022) 21, https://doi.org/10.1186/s40364-022-00372-6.

[4] T.S. Mok, Y.-L. Wu, M.-J. Ahn, M.C. Garassino, H.R. Kim, S.S. Ramalingam, F. A. Shepherd, Y. He, H. Akamatsu, W.S.M.E. Theelen, C.K. Lee, M. Sebastian, A. Templeton, H. Mann, M. Marotti, S. Ghiorghiu, V.A. Papadimitrakopoulou, Osimertinib or platinum-pemetrexed in EGFR T790M–Positive lung cancer, N. Engl. J. Med. 376 (2017) 629–640, https://doi.org/10.1056/NEJMoa1612674.

[5] A. Leonetti, S. Sharma, R. Minari, P. Perego, E. Giovannetti, M. Tiseo, Resistance mechanisms to osimertinib in EGFR-mutated non-small cell lung cancer, Br. J. Cancer 121 (2019) 725–737, https://doi.org/10.1038/s41416-019-0573-8.

[6] R. Sun, Z. Hou, Y. Zhang, B. Jiang, Drug resistance mechanisms and progress in the treatment of EGFR–mutated lung adenocarcinoma (review), Oncol. Lett. 24 (2022) 408, https://doi.org/10.3892/ol.2022.13528.

[7] J.B. Blaquier, S. Ortiz-Cuaran, B. Ricciuti, L. Mezquita, A.F. Cardona, G. Recondo, Tackling Osimertinib resistance in EGFR-mutant non-small cell lung cancer, Clin. Cancer Res. 29 (2023) 3579–3591, https://doi.org/10.1158/1078-0432.CCR-22-1912.

[8] C. Lehuédé, F. Dupuy, R. Rabinovitch, R.G. Jones, P.M. Siegel, Metabolic plasticity as a determinant of tumor growth and metastasis, Cancer Res. 76 (2016) 5201–5208, https://doi.org/10.1158/0008-5472.CAN-16-0266.

[9] H. Makinoshima, M. Takita, S. Matsumoto, A. Yagishita, S. Owada, H. Esumi, K. Tsuchihara, Epidermal growth factor receptor (EGFR) signaling regulates global metabolic pathways in EGFR-mutated lung Adenocarcinoma, J. Biol. Chem. 289 (2014) 20813–20823, https://doi.org/10.1074/jbc.M114.575464.

[10] M.J. Martin, C. Eberlein, M. Taylor, S. Ashton, D. Robinson, D. Cross, Inhibition of oxidative phosphorylation suppresses the development of osimertinib resistance in a preclinical model of EGFR-driven lung adenocarcinoma, Oncotarget 7 (2016) 86313–86325, https://doi.org/10.18632/oncotarget.13388.

[11] J.H. Kim, B. Nam, Y.J. Choi, S.Y. Kim, J.-E. Lee, K.J. Sung, W.S. Kim, C.-M. Choi, E.-J. Chang, J.S. Koh, J.S. Song, S. Yoon, J.C. Lee, J.K. Rho, J. Son, Enhanced glycolysis supports cell survival in EGFR-mutant lung Adenocarcinoma by inhibiting autophagy-mediated EGFR degradation, Cancer Res. 78 (2018) 4482–4496, https://doi.org/10.1158/0008-5472.CAN-18-0117.

[12] H. Chen, C. Lu, C. Lin, L. Li, Y. Wang, R. Han, C. Hu, Y. He, VPS34 suppression reverses osimertinib resistance via simultaneously inhibiting glycolysis and autophagy, Carcinogenesis 42 (2021) 880–890, https://doi.org/10.1093/carcin/bgab030.

[13] G. Grasmann, A. Mondal, K. Leithner, Flexibility and adaptation of cancer cells in a heterogenous metabolic microenvironment, Int. J. Mol. Sci. 22 (2021) 1476, https://doi.org/10.3390/ijms22031476.

[14] X. Hu, M. Chao, H. Wu, Central role of lactate and proton in cancer cell resistance to glucose deprivation and its clinical translation, Signal Transduct. Target. Ther. 2 (2017) 16047, https://doi.org/10.1038/sigtrans.2016.47.

[15] A. Hirayama, K. Kami, M. Sugimoto, M. Sugawara, N. Toki, H. Onozuka, T. Kinoshita, N. Saito, A. Ochiai, M. Tomita, H. Esumi, T. Soga, Quantitative metabolome profiling of colon and Stomach cancer microenvironment by Capillary electrophoresis time-of-flight mass spectrometry, Cancer Res. 69 (2009) 4918–4925, https://doi.org/10.1158/0008-5472.CAN-08-4806.

[16] K. Leithner, A. Hrzenjak, M. Trötzmüller, T. Moustafa, H.C. Köfeler, C. Wohlkoenig, E. Stacher, J. Lindenmann, A.L. Harris, A. Olschewski, H. Olschewski, PCK2 activation mediates an adaptive response to glucose depletion in lung cancer, Oncogene 34 (2015) 1044–1050, https://doi.org/10.1038/onc.2014.47.
[17] G. Bluemel, M. Planque, C.T. Madreiter-Sokolowski, T. Haitzmann, A. Hrzenjak, W. F. Graier, S.-M. Fendt, H. Olschewski, K. Leithner, PCK2 opposes mitochondrial respiration and maintains the redox balance in starved lung cancer cells, Free Radic. Biol. Med. 176 (2021) 34–45, https://doi.org/10.1016/j.freeradbiomed.2021.09.007.
[18] T.-L. Nguyen, R.v. Durán, Glutamine metabolism in cancer therapy, Cancer Drug Resist. (2018), https://doi.org/10.20517/cdr.2018.08.
[19] Y.-K. Choi, K.-G. Park, Targeting glutamine metabolism for cancer treatment, Biomol Ther (seoul) 26 (2018) 19–28, https://doi.org/10.4062/biomolther.2017.178.
[20] X. Ji, J. Qian, S.M.J. Rahman, P.J. Siska, Y. Zou, B.K. Harris, M.D. Hoeksema, I. A. Trenary, C. Heidi, R. Eisenberg, J.C. Rathmell, J.D. Young, P.P. Massion, xCT (SLC7A11)-mediated metabolic reprogramming promotes non-small cell lung cancer progression, Oncogene 37 (2018) 5007–5019, https://doi.org/10.1038/s41388-018-0307-z.
[21] K. Vanhove, E. Derveaux, G.-J. Graulus, L. Mesotten, M. Thomeer, J.-P. Noben, W. Guedens, P. Adriaensens, Glutamine addiction and therapeutic strategies in lung cancer, Int. J. Mol. Sci. 20 (2019) 252, https://doi.org/10.3390/ijms20020252.
[22] C. Hodakoski, B.D. Hopkins, G. Zhang, T. Su, Z. Cheng, R. Morris, K.Y. Rhee, M. D. Goncalves, L.C. Cantley, Rac-mediated macropinocytosis of Extracellular protein promotes glucose Independence in non-small cell lung cancer, Cancers (basel) 11 (2019) 37, https://doi.org/10.3390/cancers11010037.
[23] S. La Monica, D. Madeddu, M. Tiseo, V. Vivo, M. Galetti, D. Cretella, M. Bonelli, C. Fumarola, A. Cavazzoni, A. Falco, A. Gervasi, C.A. Lagrasta, N. Naldi, E. Barocelli, A. Ardizzoni, F. Quaini, P.G. Petronini, R. Alfieri, Combination of gefitinib and pemetrexed prevents the acquisition of TKI resistance in NSCLC cell lines Carrying EGFR- activating mutation, J. Thorac. Oncol. 11 (2016) 1051–1063, https://doi.org/10.1016/j.jtho.2016.03.006.
[24] S. La Monica, R. Minari, D. Cretella, M. Bonelli, C. Fumarola, A. Cavazzoni, M. Galetti, G. Digiacomo, F. Riccardi, P.G. Petronini, M. Tiseo, R. Alfieri, Acquired BRAF G469A mutation as a resistance mechanism to first-line Osimertinib treatment in NSCLC cell lines Harboring an EGFR exon 19 deletion, Target Oncol. 14 (2019) 619–626, https://doi.org/10.1007/s11523-019-00669-x.
[25] S. La Monica, R. Minari, D. Cretella, L. Flammini, C. Fumarola, M. Bonelli, A. Cavazzoni, G. Digiacomo, M. Galetti, D. Madeddu, A. Falco, C.A. Lagrasta, A. Squadrilli, E. Barocelli, A. Romanel, F. Quaini, P.G. Petronini, M. Tiseo, R. Alfieri, Third generation EGFR inhibitor osimertinib combined with pemetrexed or cisplatin exerts long-lasting anti-tumor effect in EGFR-mutated pre-clinical models of NSCLC, J. Exp. Clin. Cancer Res. 38 (2019) 222, https://doi.org/10.1186/s13046-019-1240-x.
[26] M. Mancini, H. Gal, N. Gaborit, L. Mazzeo, D. Romaniello, T.M. Salame, M. Lindzen, G. Mahlknecht, Y. Enuka, D.G. Burton, L. Roth, A. Noronha, I. Marrocco, D. Adreka, R.E. Altstadter, E. Bousquet, J. Downward, A. Maraver, V. Krizhanovsky, Y. Yarden, An oligoclonal antibody durably overcomes resistance of lung cancer to third-generation <scp>EGFR</scp> inhibitors, EMBO Mol. Med. 10 (2018) 294–308, https://doi.org/10.15252/emmm.201708076.
[27] M. Bonelli, R. Terenziani, S. Zoppi, C. Fumarola, S. La Monica, D. Cretella, R. Alfieri, A. Cavazzoni, G. Digiacomo, M. Galetti, P.G. Petronini, Dual inhibition of CDK4/6 and PI3K/AKT/mTOR signaling impairs energy metabolism in MPM cancer cells, Int. J. Mol. Sci. 21 (2020) 5165, https://doi.org/10.3390/ijms21145165.
[28] A. Al Mamun, H. Hayashi, A. Yamamura, M.J. Nayeem, M. Sato, Hypoxia induces the translocation of glucose transporter 1 to the plasma membrane in vascular endothelial cells, J. Physiol. Sci. 70 (2020) 44, https://doi.org/10.1186/s12576-020-00773-y.
[29] A. Cavazzoni, R.R. Alfieri, C. Carmi, V. Zuliani, M. Galetti, C. Fumarola, R. Frazzi, M. Bonelli, F. Bordi, A. Lodola, M. Mor, P.G. Petronini, Dual mechanisms of action of the 5-benzylidene-hydantoin UPR1024 on lung cancer cell lines, Mol. Cancer Ther. 7 (2008) 361–370, https://doi.org/10.1158/1535-7163.MCT-07-0477.
[30] C. Fumarola, S. La Monica, R.R. Alfieri, E. Borra, G.G. Guidotti, Cell size reduction induced by inhibition of the mTOR/S6K-signaling pathway protects jurkat cells from apoptosis, Cell Death Differ. 12 (2005) 1344–1357, https://doi.org/10.1038/sj.cdd.4401660.
[31] S. La Monica, M. Galetti, R.R. Alfieri, A. Cavazzoni, A. Ardizzoni, M. Tiseo, M. Capelletti, M. Goldoni, S. Tagliaferri, A. Mutti, C. Fumarola, M. Bonelli, D. Generali, P.G. Petronini, Everolimus restores gefitinib sensitivity in resistant non-small cell lung cancer cell lines, Biochem. Pharmacol. 78 (2009) 460–468, https://doi.org/10.1016/j.bcp.2009.04.033.
[32] Y.C. Long, AMP-activated protein kinase signaling in metabolic regulation, J. Clin. Investig. 116 (2006) 1776–1783, https://doi.org/10.1172/JCI29044.
[33] T. Boch, J. Köhler, M. Janning, S. Loges, Targeting the EGF receptor family in non-small cell lung cancer—increased complexity and future perspectives, Cancer Biol. Med. 19 (2022) 1543–1564, https://doi.org/10.20892/j.issn.2095-3941.2022.0540.
[34] S.Y. Hong, F.-X. Yu, Y. Luo, T. Hagen, Oncogenic activation of the PI3K/Akt pathway promotes cellular glucose uptake by downregulating the expression of thioredoxin-interacting protein, Cell. Signal. 28 (2016) 377–383, https://doi.org/10.1016/j.cellsig.2016.01.011.
[35] C. Fumarola, P.G. Petronini, R. Alfieri, Impairing energy metabolism in solid tumors through agents targeting oncogenic signaling pathways, Biochem. Pharmacol. 151 (2018) 114–125, https://doi.org/10.1016/j.bcp.2018.03.006.
[36] E. Pranzini, E. Pardella, P. Paoli, S.-M. Fendt, M.L. Taddei, Metabolic reprogramming in anticancer drug resistance: a focus on amino acids, trends, Cancer 7 (2021) 682–699, https://doi.org/10.1016/j.trecan.2021.02.004.
[37] S. Kim, J.S. Jeon, Y.J. Choi, G.H. Baek, S.K. Kim, K.W. Kang, Heterogeneity of glutamine metabolism in acquired-EGFR-TKI-resistant lung cancer, Life Sci. 291 (2022) 120274, https://doi.org/10.1016/j.lfs.2021.120274.
[38] M. Momcilovic, S.T. Bailey, J.T. Lee, M.C. Fishbein, C. Magyar, D. Braas, T. Graeber, N.J. Jackson, J. Czernin, E. Emberley, M. Gross, J. Janes, A. Mackinnon, A. Pan, M. Rodriguez, M. Works, W. Zhang, F. Parlati, S. Demo, E. Garon, K. Krysan, T.C. Walser, S.M. Dubinett, S. Sadeghi, H.R. Christofk, D. B. Shackelford, Targeted inhibition of EGFR and glutaminase induces metabolic crisis in EGFR mutant lung cancer, Cell Rep. 18 (2017), https://doi.org/10.1016/j.celrep.2016.12.061.
[39] A.P.J. van den Heuvel, J. Jing, R.F. Wooster, K.E. Bachman, Analysis of glutamine dependency in non-small cell lung cancer, Cancer Biol. Ther. 13 (2012) 1185–1194, https://doi.org/10.4161/cbt.21348.
[40] R.U. Svensson, R.J. Shaw, Tumour friend or foe, Nature 485 (2012) 590–591, https://doi.org/10.1038/485590a.
[41] H. Endo, S. Owada, Y. Inagaki, Y. Shida, M. Tatemichi, Metabolic reprogramming sustains cancer cell survival following extracellular matrix detachment, Redox Biol. 36 (2020) 101643, https://doi.org/10.1016/j.redox.2020.101643.
[42] B. Faubert, K.Y. Li, L. Cai, C.T. Hensley, J. Kim, L.G. Zacharias, C. Yang, Q.N. Do, S. Doucette, D. Burguete, H. Li, G. Huet, Q. Yuan, T. Wigal, Y. Butt, M. Ni, J. Torrealba, D. Oliver, R.E. Lenkinski, C.R. Malloy, J.W. Wachsmann, J.D. Young, K. Kernstine, R.J. DeBerardinis, Lactate metabolism in human lung tumors, Cell 171 (2017) 358–371.e9, https://doi.org/10.1016/j.cell.2017.09.019.
[43] K.E. Pendleton, K. Wang, G.V. Echeverria, Rewiring of mitochondrial metabolism in therapy-resistant cancers: permanent and plastic adaptations, Front. Cell Dev. Biol. 11 (2023), https://doi.org/10.3389/fcell.2023.1254313.